SC/Morgan

RCA VICTOR RESEARCH REPORT
7-801-38

TIME HISTORY OF THE MAGNETOSPHERIC CAVITY

F.J.F. Osborne
M.P. Bachynski
J.V. Gore

JUNE 1965

Prepared Under

Contract PD69-400007, Serial 2PD4-5

of the

DEFENCE RESEARCH BOARD OF CANADA

and

NASA Contract NAS_W 1088

RCA VICTOR COMPANY, LTD.
RESEARCH LABORATORIES
MONTREAL, CANADA

TIME HISTORY OF THE MAGNETOSPHERIC CAVITY *

F.J.F. Osborne, M.P. Bachynski, J.V. Gore
RCA Victor Research Laboratories
Montreal, Canada

- ABSTRACT -

14961

Scale model laboratory experiments simulating the effect of the solar wind on the magnetosphere have shown the time history of the formation and breakup of the magnetospheric cavity. Time resolved (1 μsec) data on the visible "standoff" interaction show that the "quasi Van Allen belts" first become visible well within the cavity at the time the plasma wind encounters the fringing terrella field. The belts at this time show a definite structure with "ribbons" of plasma along the field lines. This structure is probably associated with oscillatory phenomena present in the belts and their excitation mechanism. The polar views show considerable asymmetry of both the internal and external phenomena throughout the interaction. The visual asymmetries indicate that the plasma in the tail of the dipole magnetic field "wags" as the interaction builds up and decays. Magnetic field measurements in the equatorial plane show a similar motion of the magnetic field in the tail. Author

---

* Paper presented URSI Spring Meeting, Washington, D.C. (1965).

INTRODUCTION

A strong interaction occurs when the solar wind or plasma ejected from the sun streams into interplanetary space and encounters the magnetic field of the earth. This interaction results in a distortion of the earth's magnetic field both in space and at the earth's surface (magnetic storm) and numerous other complex natural phenomena. The complex nature of the interaction makes it extremely difficult to sort out the crucial mechanisms contributing to the numerous observed effects.

In an effort to try to get a better understanding of some of the phenomena involved in order to account for the observations made both by space craft and from the earth resort has been made to laboratory experiments based on scaled models. (Osborne et al 1963, 1964, 1964a, 1964b). The experiments consist of propelling a stream of plasma with a plasma gun into the vicinity of a three-dimensional dipole magnetic field and studying the interaction. Previous results of such experiments in which plasma has been shot at the equatorial plane of the magnetic field have shown:

(i) a stand-off of plasma at approximately the position where the kinetic pressure of the solar wind is balanced by the magnetic pressure of the dipole magnetic field

(ii) the sweeping of the magnetic field and the formation of the front side of the magnetospheric cavity (in agreement with space measurements)

(iii) the formation of trapped regions of plasma similar in shape and position to the natural Van Allen belts, and which exhibit oscillatory phenomena (Osborne et al 1964)

(iv) weakly trapped regions of plasma in the vicinity of the polar regions

(v) the motion of the "dip" pole under the influence of the plasma

(vi) a westward motion of the plasma in the simulated Van Allen belts

(vii) the dependence of penetration of plasma into the polar regions on the properties of the solar wind

This paper, after considering various aspects of the relevant parameters involved in the scaling presents new results showing the time history of the formation and decay of the magnetospheric cavity and associated phenomena under the action of a "gust" of solar wind.

CONSIDERATIONS OF SOME RELEVANT PARAMETERS

The major considerations of the scaling requirements pertaining to a model experiment on the interaction between the solar wind and the magnetsphere have been considered previously (Shkarofsky (1962), Bachynski (1964) and Shkarofsky (to be published)). It seems worthwhile however, to treat in detail the relative magnitudes of some of the parameters involved as well as several other key aspects. This section will therefore be devoted to several such topics namely the cyclotron radius, the magnetospheric boundary at the equatorial plane and the Debye length.

(a) The Cyclotron Radius

The cyclotron radius (r_b) for a charged particle gyrating in a magnetic field (B) is given by:

$$r_b = \frac{v_t}{\omega_b} = 5.68\times10^{-8}\ v_t\ m_o/B \quad \text{cm} \qquad (1)$$

where v_t is the thermal velocity of the particle in cm/sec

ω_b is the cyclotron frequency for the given particle

m_o is the mass of the particle in electron mass units i.e.

$m_o = 1$ for an electron, $m_o = 1836.6$ for a proton, etc.

B is the magnetic field in gauss.

The variation of cyclotron radius with magnetic field strength, thermal velocity and mass (species) is shown in Figure 1. The regime of space parameters and laboratory parameters are indicated in the Figure. In relation to the current model experiments, typical values of the cyclotron radius for a typical thermal velocity of 10^5 cm/sec are given in Table I.

As can be seen, the electron cyclotron radius is exceedingly small. Previous experiments show from spectroscopic data that oxygen ions are trapped within the cavity. Here the magnetic fields are in the kilogauss range corresponding to an ion cyclotron radius of a few millimeters. Hence "mirroring" of the charged particles trapped in the dipole field of the terrella should take place. At the boundary of the magnetospheric cavity, the incoming plasma is seeded with barium ions with a resulting cyclotron radius of several centimeters. However, as shown in the next section, the boundary thickness is determined more by the electrons than the ions and therefore this relatively large ion cyclotron radius has a secondary effect on the scaling.

(b) The Boundary

(i) The Sheath Thickness

The main features of one model of an idealized plasma-magnetic field interface has been considered among others by Ferraro (1952), Rosenbluth (1963), Grad (1961), Colgate (1961), Scarf (1964) and Sesters (1965). In this simple two-dimensional case, one can consider plasma streaming at right angles to a magnetic field (see Fig.2). This can be considered analogous to the solar wind

being incident along the equatorial plane where the earth's magnetic field is transverse to the flow. The main features of the particle trajectories are discussed in the aforementioned references and will only be summarized here. The ions with their larger mass (and hence greater kinetic energy) tend to penetrate further into the magnetic field than the electrons. This charge separation gives rise to an electric field (E_s) which accelerates the electrons in the $\bar{E}_s \times \bar{B}$ direction and therefore causes them to execute broader turns. Simultaneously, the ions lose energy until they are finally turned around quite sharply. In fact, considerations of conservation of particle energy and momentum require that the ions and electrons exchange energy momentarily, but regain their original energies as they leave the interface or sheath. Thus the ions determine the depth of penetration but the electric field due to charge separation determines the final particle trajectories. (This streaming of electrons as found in the boundary sheath is known to give rise to instabilities. However, dissipation of energy due to collisional effects or the fact that the magnetospheric boundary is curved not planar, may present the growth of such instabilities.)

The different depths of penetration of the electrons and ions results in a transition region or sheath of thickness δ where:

$$\delta = c/\omega_p = 5.32\times10^5/\sqrt{n} \quad \text{cm} \tag{2}$$

where c is the velocity of light

ω_p is the plasma frequency

n is the charge particle number density (cm^{-3})

Thus in the simple case the sheath thickness depends solely on the charge particle number density.

Equation (2) can be put in several different forms. Thus for a <u>thermal</u>, non-streaming plasma, the balance conditions between the thermal pressure and magnetic pressure require that:

$$nkT = B^2/2\mu_o \tag{3}$$

where κ is Boltzmann's constant

T is the electron temperature (^{o}K)

B is the magnetic field

μ_o is the permeability of free space

Using the fact that the electron thermal velocity $v_t = (2\kappa T/m_e)^{\frac{1}{2}}$ where m_e is the electron mass, we can write:

$$\delta = v_t/\omega_b = 3.38V^{\frac{1}{2}}/B \quad \text{cm} \tag{4}$$

(V is the electron temperature in electron volts, B is magnetic field in gauss)

Thus we see that the sheath thickness for a thermal non-streaming plasma is of the order of the <u>electron</u> cyclotron radius.

For a streaming plasma (streaming velocity considerably exceeds the thermal velocity), the balance conditions require that: (considering specular reflection at the boundary)

$$2n(m_i + m_e)V_o^2 = B^2/2\mu_o \tag{5}$$

where: m_i is the ion mass

V_o is the streaming velocity.

Using this expression, the sheath thickness can be written:

$$\delta = \frac{\sqrt{2}\, V_o}{\omega_{be} \sqrt{\frac{m_e}{m_i}}}$$

where: $\omega_{be} = \frac{eB}{m_e}$ the electron cyclotron frequency.

Typical values for the parameters at the magnetospheric boundary are: $B \sim 10^{-3}$ gauss, $V_o \sim 500$ km/sec, $n \sim 1$-10 particles/cm^3, ions are protons so that $\sqrt{m_e/m_i} \sim \frac{1}{42.8}$. This gives typical sheath thickness estimates of:

$$\delta \sim 1\text{-}5 \text{ km}$$

(A more complete sheath theory (Scarf (1964)) which considers fluctuating fields and hot electrons in the sheath give sheath thicknesses of the order of 70 km.)

Typical laboratory values are: B ~ 50-500 gauss at boundary, $V_0 \sim 2\times10^6$ cm/sec, $n \sim 10^{12} - 10^{13}$ particles/cm^3, ions are barium (atomic weight 136). This leads to sheath thickness values of

$$\delta \sim 0.1 - 1 \text{ cm}$$

As reported previously (Osborne et al 1964b) magnetic boundaries as thin as 3 mm have been observed experimentally.

(ii) Boundary Postion

Equation (5) gives the magnetic field value B at the stand-off position and can be exressed as:

$$nAV_0^2 = 1.18\times10^{22}B^2 \tag{7}$$

where: A is the mass number of the ion species and n is in particles/cm^3, V_0 in cm/sec and B in gauss. Normally the magnetic field B_0 at any location r_0 on the equatorial plane varies in a dipole fashion namely:

$$B_0 = B_E \left(\frac{R_E}{r_0}\right)^3$$

where: B_E and R_E are the magnetic field values and radius at the equator respectively.

Due to the streaming plasma, the magnetic field at the location r_0 will be increased from its value B_0 to some value αB_0. If we assume that the field is still approximately dipole in configuration the field at the boundary position (B) or equivalently the location of the boundary position (r_0) can be determined by considering a dipole field whose field value at the equator has been increased by a value α, i.e.

$$\frac{r_0}{R_E} = \left(\frac{\alpha B_E}{B}\right)^{1/3} \tag{8}$$

where: α is the factor by which the unperturbed field at position r_o has been increased at the stand-off position (usually $\alpha \sim 2$).

From Equation (8) and (7)

$$\frac{r_o}{R_E} = \left[\frac{(\alpha B_E)^2}{2\mu_o} \frac{1}{2nm_i V_o^2}\right]^{1/6} \tag{9}$$

In the natural situation, taking $n \sim 5/cm^3$, $V_o = 500$ km/sec, $\alpha \sim 2$, protons, $B_E = 0.312$ gauss yields: $B \sim 10^{-3}$ gauss, $r_o/R_E \sim 8.5$.

In the laboratory α, V_o, r_o/R_E, B_E and B can be measured directly (Osborne et al (1964b)). Hence Equation (7) can be used to determine the electron density and Equation (8) as a check on the boundary position. A typical value is: B = 250 gauss, A = 136, $V_o = 2\times10^6$ cm/sec. This leads to $n \sim 10^{12}$ particles/cm^3. The boundary positions agree within the accuracy to which it is possible to measure α and B.

(c) Debye Length

An indication of the charge separation effects is given by the Debye length (λ_D), namely:

$$\lambda_D = 0.69 \sqrt{T/n} \text{ cm} \tag{10}$$

Typical laboratory values are: ($n = 10^{11} - 10^{13}/cm^3$, $T \sim 30{,}000^0$)

$$\lambda_D \sim 10^{-4} - 10^{-5} \text{ cm}$$

In space: ($n \sim 10^0 - 10/cm^3$, $T \sim 1{,}000^0$)

$$\lambda_D \sim .1 - 1\text{m}$$

(d) Discussion

Of pertinence to the scaling is a comparison of the ratios of various parameters in the natural situation to those in the laboratory. In relationship to the thickness of the magnetospheric boundary a dimensionless parameter which may be of importance is the sheath thickness compared to the ion cyclotron

radius (r_{bi}). For an ion thermal velocity of V_t we have:

$$\frac{\text{sheath thickness}}{\text{ion cyclotron radius}} = \delta/r_{bi} = \frac{e}{\omega_p} \cdot \frac{\omega_{bi}}{V_t}$$

A typical laboratory value: $V_t \sim 2\times10^5$ cm/sec, $n = 10^{12}/cm^3$, m_i = 136 times the proton mass, B ~ 200 gauss at the boundary.

For these parameters: $\delta/r_{bi} \tilde{=} 0.02$

For a magnetic field increased by a factor 10, $\delta/r_{bi} \sim 0.2$ [Values in the laboratory can range from 0.01 to 10.]

In space if we take $V_t \sim 10^8$ cm/sec, $n \sim 4/cm^3$, m_i = mass of proton, $B \sim 10^{-3}$ gauss

$$\delta/r_{bi} \sim 0.025$$

[Values in space can range over 0.01 to 100]

Thus in both cases this ratio is not that far different. (The use of lighter ions in the laboratory experiment would also alter this ratio.)

We also note that both the ion cyclotron radius and the sheath thickness are many Debye lengths in extent. This is true both in space and in the laboratory. It is therefore evident that similar mechanisms may be operative in the laboratory scale model experiments as in the natural situation.

TIME HISTORY OF MAGNETOSPHERE

The time history of the formation and decay of the magnetospheric cavity under the action of a "gust" of solar wind is illustrated in a series of photographs taken with a 1 microsecond exposure at predetermined times after the launching of the plasma simulating the solar wind. Figure 3 illustrates the plasma formation as viewed from the sunrise equatorial position. The views from above the polar axis are shown in Figure 4. The measurements made at

identical times should be considered simultaneously in ascertaining the time history of the interaction between the solar wind plasma and the three-dimensional dipole of the model earth or terrella.

The important features of the buildup and collapse of the magnetospher cavity to note are:

1. With reference to Figures 3 and 4 it is apparent that 15 μsec after launching the plasma from the solar wind "gun" there is no visible plasma in the vicinity of the terrella. The first indication of plasma occurs at 17μsec - a diffuse trapped region on the windward side of the terrella showing pronounced striations or periodic structure when seen from the polar axis. (Some plasma at this same time penetrates into the polar regions.) The situations show a periodicity of about 0.6 cm or wavelength of 1.2 cm. Hence we can consider a disturbance with a wavelength of the order of a centimetre. Calculating the order of magnitude of the Alfven velocity V_A for these conditions,

$$V_A = \frac{B}{\sqrt{\mu_o \, nm_i}} = \frac{2.2\times10^{11}B}{\sqrt{nA}} \text{ cm/sec} \qquad (11)$$

and taking: $B \sim 100$ gauss, $A = 32$, $n \sim 10^{12}/cm^3$ we arrive at

$$V_A \sim 4\times10^6 \text{ cm/sec.}$$

This would correspond to a disturbance with frequency f_A given by:

$$f_A = V_A/\lambda_A = 4\times10^6/1.2 \sim 3.3 \text{ Mc/sec}$$

It may be noted that this Alfven velocity is calculated for the position of the interior phenomena and will represent the highest velocity (highest B) experienced to this point by a wave initiated at the moving front, assuming that the density is constant over the volume.

Both electrical probe and magnetic probe measurements in the plasma in this region show pronounced signal fluctuations at discrete frequencies (Osborne et al 1964). The frequency of these fluctuations are in the 100 Kc to 1 Mc range. It therefore appears that these fluctuations and striations could be due to a magnetohydrodynamic wave which is generated as the plasma first strikes the outer edge of the dipole field. (Although at these times the incoming plasma from the plasma gun is not visible in the field of view, magnetic measurements show that this plasma has already struck the outer magnetic field of the terrella).

2. This interior region becomes better defined (indicating a definite trapping mechanism in the dipole magnetic field), shearing into two regions as seen from the poles) diffusing the striations and exhibiting a distinct westward motion. (The diffusing of the striations may be due to the fact that the incoming plasma continues to move against the dipole magnetic field and thus various magnetohydrodynamic wave modes may be excited so that no single periodicity is now possible.) This plasma whose distribution resembles that of the Van Allen belts in space is formed entirely by precursor radiation from the plasma gun at a time considerably in advance of the main stream of plasma which only becomes visible at 23 μsec from the time of launching.

3. The solar wind plasma as it arrives, compresses the dipole field (see the 25 and 27 μsec photographs) moving the magnetospheric boundary and the Van Allen belt position nearer towards the terrella. At 33 to 39 μsec, equilibrium appears to have been achieved after which time the solar wind plasma decreases in pressure.

4. Regions of plasma become trapped in the polar regions (in addition to the simulated Van Allen belts) in the interaction times 29-45 μsec. As seen from the polar view, this plasma forms a "tail" trying to encircle the terrella (in addition to the westward motion with increasing time of the interaction).

5. At about the 45 μsec time, the solar wind plasma eases its pressure. This is accompanied by a very dramatic change in the plasma trapped in the vicinity of the terrella. The plasma originally trapped in the polar regions is now absent. The plasma in the magnetospheric cavity begins to break up into a complicated structure. There is a precipitation of plasma into the polar regions in a ring structure around the dip pole (note particularly the 51 μsec polar view).

6. At late times (> 54 μsec) the "belt" structure diffuses, leaving principally the plasma trapped in the simulated Van Allen belts which lasts for a long time (> 75 μsec).

Another feature which has been measured by different techniques is equally noteworthy. The component of the magnetic field measured in the equatorial plane at the time of maximum magnetic field compression (~ 33 μsec) is shown in Fig. 5. This plot shows a magnetic field "tail" of the magnetospheric cavity swung about 60° westward from the wind direction in agreement with the visible plasma "tail" shown earlier. Since with very little solar wind pressure, the backside of the magnetosphere must be nearly directly behind the windward direction, this implies a "wag" of the magnetospheric tail during the interaction of the solar wind. The asymmetry of the earth's magnetic field in the equatorial plane is also apparent from the above plot. Some indication of an asymmetry in the earth's magnetospheric cavity has been given by Obayashi (1964) although

space data on this point are as yet very meagre. (Dessler and Walters (1964)) have discussed a "wag" of the magnetospheric tail but their mechanism is different than that which could be acting here.)

SUMMARY

Detailed examination has been made of the processes occurring within the boundary region of a scaled interaction between the solar wind and the earth's magnetic dipole field. It has been shown that the pertinent parameters of Debye length, Rosenbluth sheath criterion (c/ω_p) and the ion cyclotron radii are of approximately the same relative magnitude for both the geophysical and laboratory situations. Thus under similar plasma regimes, the same types of processes may be expected to occur.

Whereas in space, measurements of magnetospheric boundary thickness are complicated by boundary fluctuations and satellite motion, the laboratory measurements clearly indicate a Rosenbluth sheath mechanism rather than direct control by the ion cyclotron radius.

Time resolved data on the visible features of a "standoff" interaction show that the quasi Van Allen belts exhibit the first luminosity and are also of long persistence. The period of initial generation of these belts shows considerable structure. The periodicity of this structure in conjunction with the oscillatory phenomena previously reported suggests an mhd wave perturbation.

Regions of plasma nominally trapped within the magnetosphere in the region of the neutral points have been found to be precipitated out on the terrella surface at specific times of the interaction and to appear on the surface as a ring of luminosity approximately centered on the dip-poles.

The polar view of the magnetosphere shows considerable asymmetry of both the internal and external phenomena. These asymmetries vary with time and thus generate a "wag" of the magnetospheric tail. These data are confirmed by magnetic measurements in the equatorial plane.

ACKNOWLEDGEMENTS

This work was done under Contract PD69-400007 Serial 2PD4-5 of the Defence Research Board of Canada and NASA Contract NASw 1088.

REFERENCES

Bachynski, M.P. (1964), Simulation of geophysical phenomena in the laboratory, AIAA Jour. 2 1873-1882.

Colgate, S.A. (1961), Ionization in crossed electric and magnetic fields in Electromagnetics and Fluid Dynamics of Gaseous Plasma, ed. J.Fox, Polytechnic Press, N.Y. 1961, 373-386.

Dessler, A.J. and G.K. Walters (1964), Hydromagnetic coupling between solar wind and magnetosphere, Planet Space Sci. 12, 227-234.

Ferraro, V.C.A. (1952), On the theory of the first phase of a geomagnetic storm: a new illustrated calculation based on an idealized (plane not cylindrical) model field distribution. J.Geophys.Res. 57, 15.

Grad, H. (1961), Boundary layer between a plasma and a magnetic field, Phys. Fluids 4, 1366-1375.

Obayashi, T. (1964), Magnetosphere and its boundary, Report of Ionosphere and Space Research in Japan XVIII, No.3, 228-234.

Osborne, F.J.F., I.P. Shkarofsky and J.V. Gore (1963), Laboratory simulation of the solar wind magnetosphere interaction, Can.J.Phys. 41, 1747-1752.

Osborne, F.J.F., M.P. Bachynski and J.V. Gore (1964), Oscillatory phenomena in the laboratory simulation of the magnetosphere. Symposium on Ultra Low Frequency Electromagnetic Fields. Boulder, Colarado, Aug.17-20.

Osborne, F.J.F., M.P. Bachynski and J.V. Gore (1964a), Laboratory measurements of plasma trapping within the magnetosphere, Appl.Phys.Letters 5, 77-79.

Osborne, F.J.F., M.P. Bachynski and J.V. Gore (1964b), Laboratory studies of the variation of the magnetosphere with solar wind properties. J.Geophys. Res. 69, 4441-4449.

Rosenbluth, M. (1963), Surface layer model in the limit of no collisions, Plasma Physics and Thermonuclear Research, J.L. Tuck, W.B. Thompson, editors, Pergamon Press Inc. London. 271-277.

Scarf, F.L. (1964), The solar wind and its interaction with magnetic fields, Space Physics, D.P. LeGalley, A.Rosen editors, J. Wiley and Sons Inc. New York 437-473.

Sestero, A. (1965), Charge separation effects in the Ferraro-Rosenbluth cold plasma sheath model, Phys.Fluids 8 739-744.

Shkarofsky, I.P. (1962), The solar wind, the magnetosphere and their simulation in the laboratory, RCA Victor Company, Research Report 7-801-22.

Shkarofsky, I.P. (To be published), Laboratory simulation of disturbances produced by bodies moving through a plasma and of other geophysical phenomena. Astronautica Acta.

B (gauss)	r_b (electrons)	r_b (O_2 ion)	r_b (B_a ion)
200 at boundary	2.8×10^{-5} cm	1.7 cm	7.1 cm
1,000 inside magnetosphere	5.7×10^{-6} cm	0.33 cm	1.4 cm

Table I

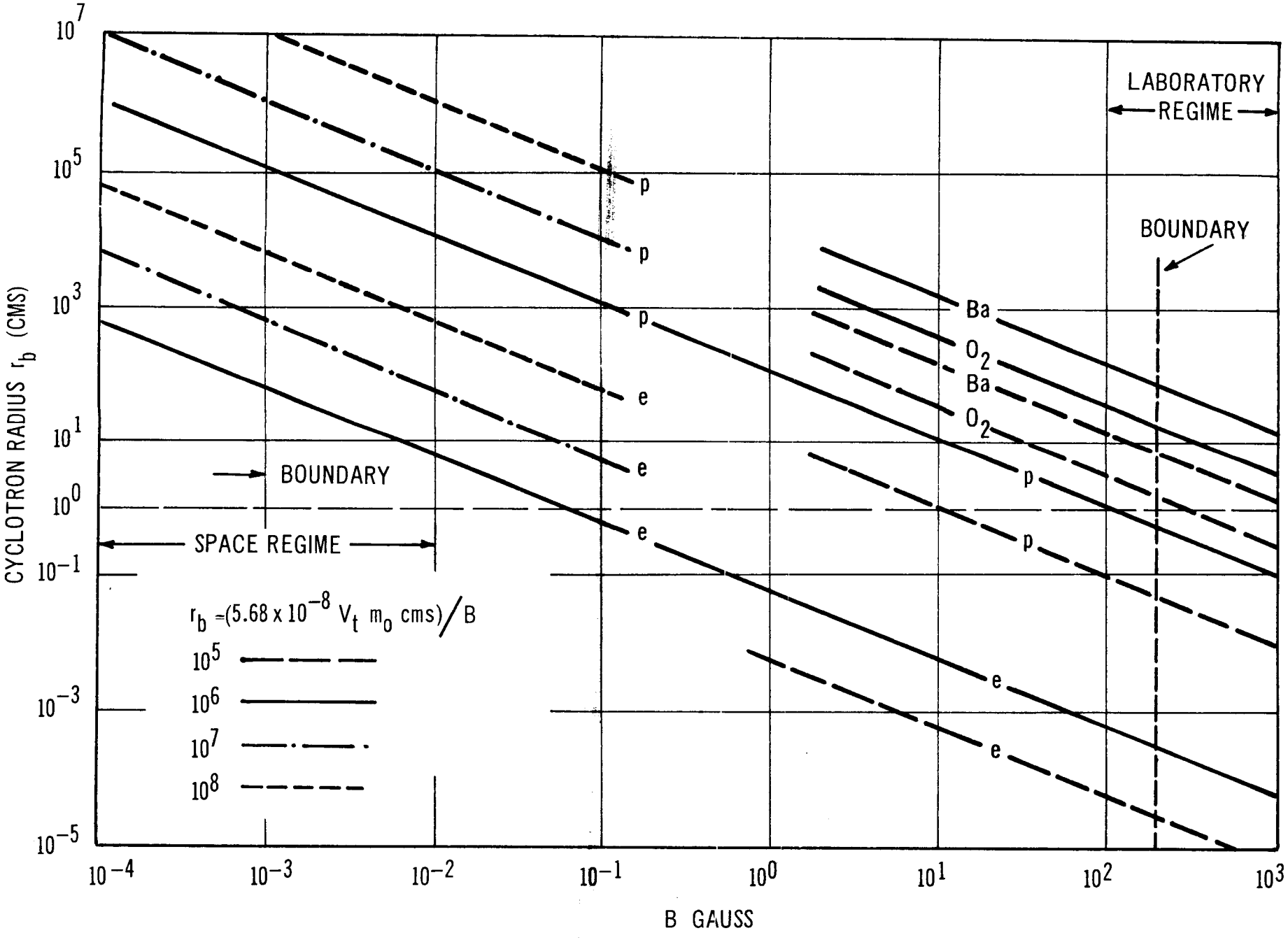

Figure 1 – The variation of cyclotron radius with magnetic field strength, thermal velocity and mass

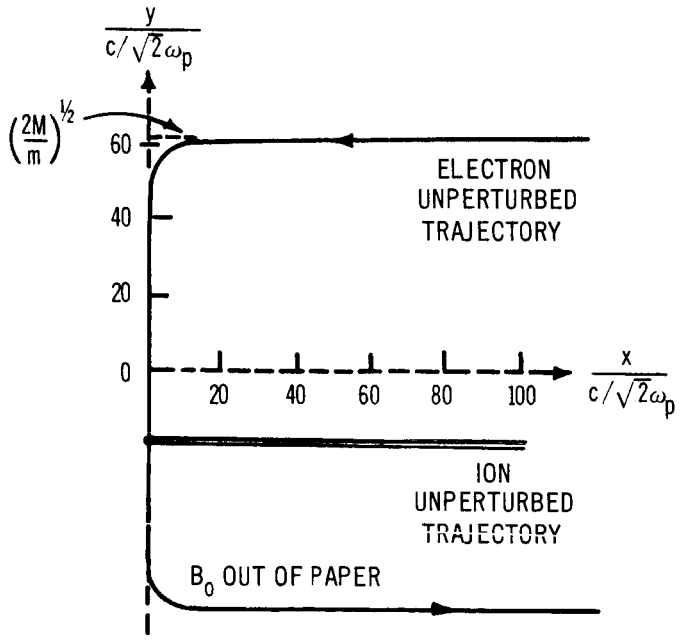

Figure 2 – The idealized electron and trajectories in a plasma-magnetic field interface

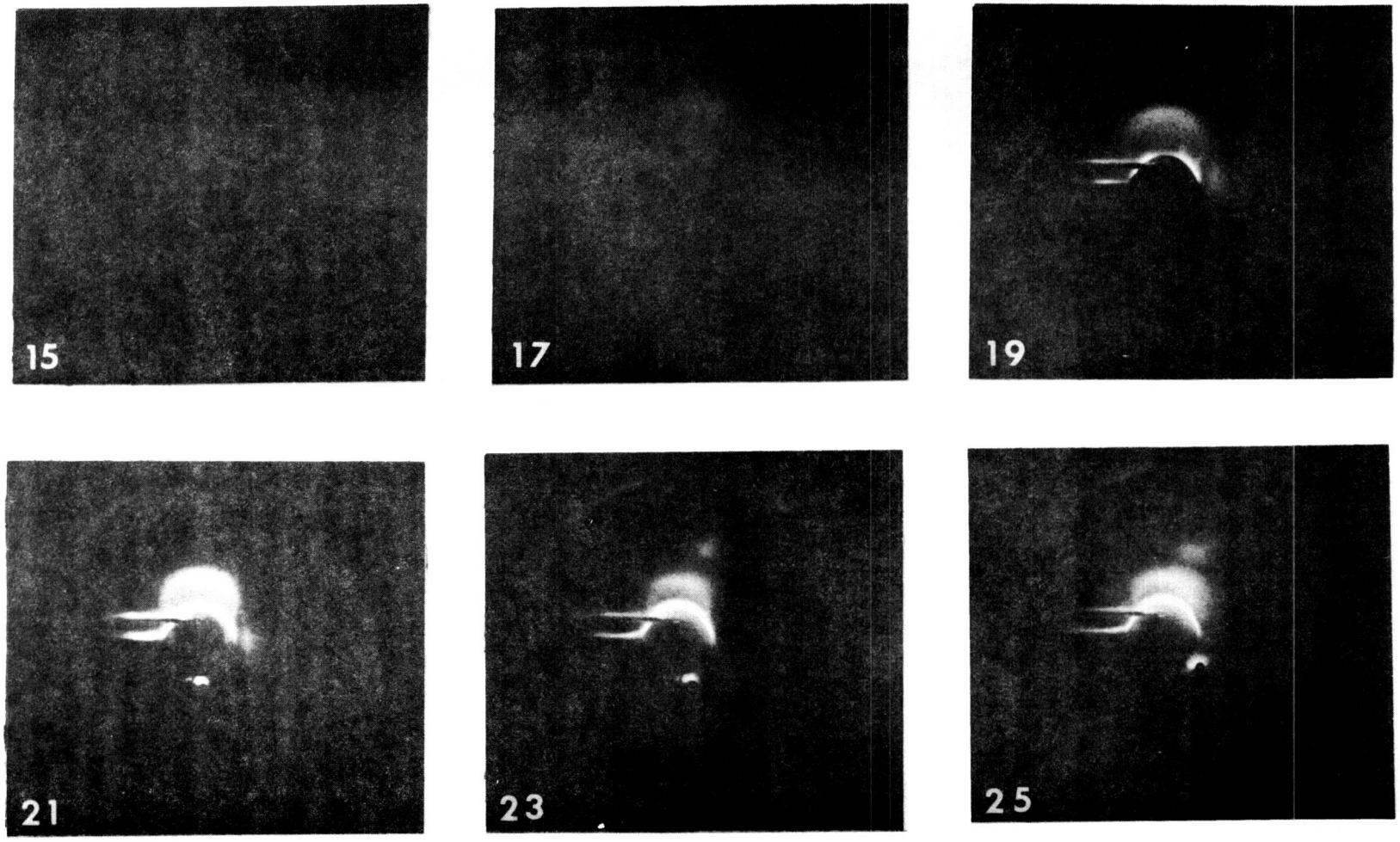

View from sunrise equatorial position of Solar Wind Magnetosphere Interaction. 1 μsec exposures. Numbers refer to time in microseconds from bank firing. Wind incident from top. Primary bank energy 1.7 kilojoules.

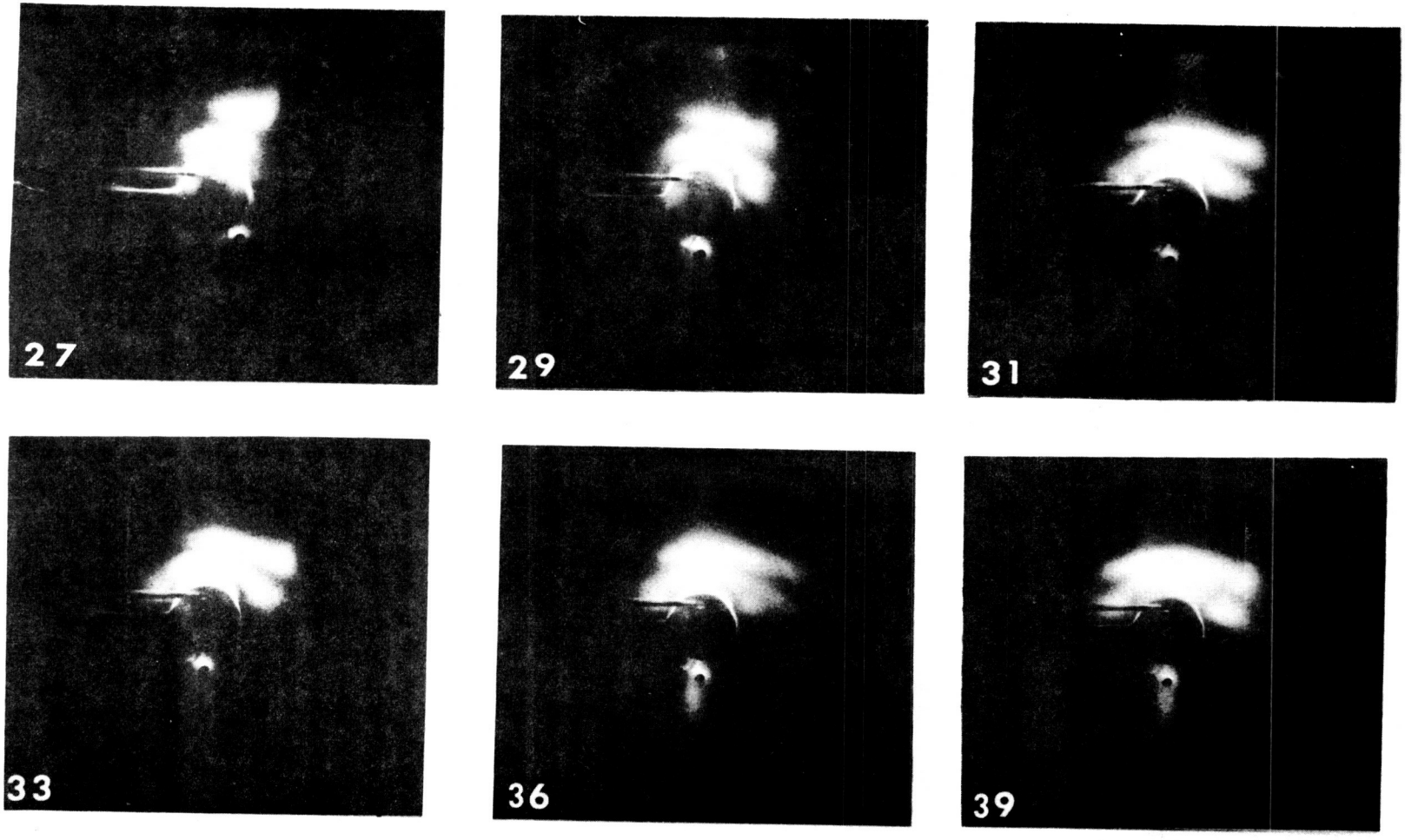

View from sunrise equatorial position of Solar Wind Magnetosphere Interaction. 1 μsec exposures. Numbers refer to time in microseconds from bank firing. Wind incident from top. Primary bank energy 1.7 kilojoules.

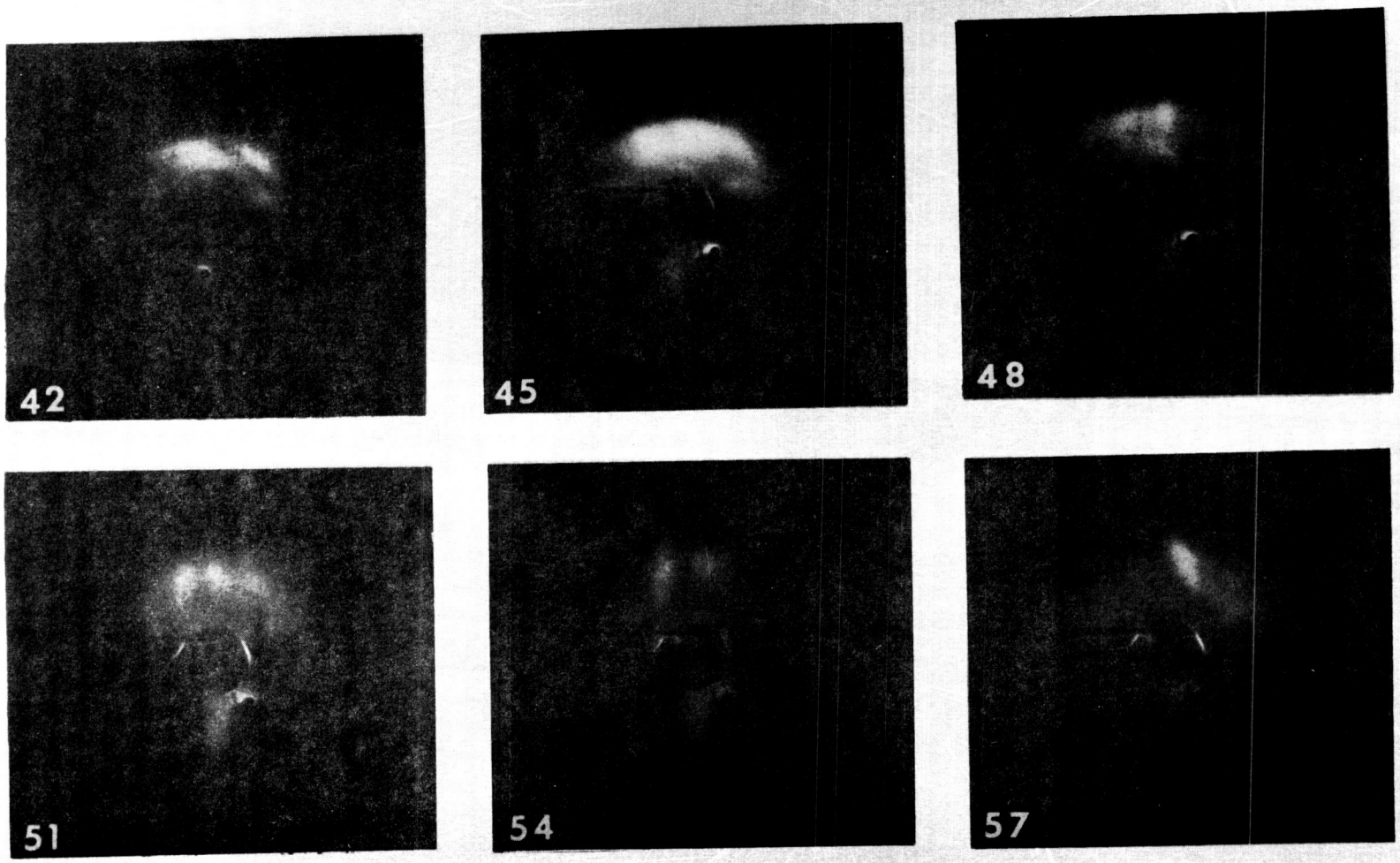

View from sunrise equatorial position of Solar Wind Magnetosphere Interaction. 1 μsec exposures. Numbers refer to time in microseconds from bank firing. Wind incident from top. Primary bank energy 1.7 kilojoules.

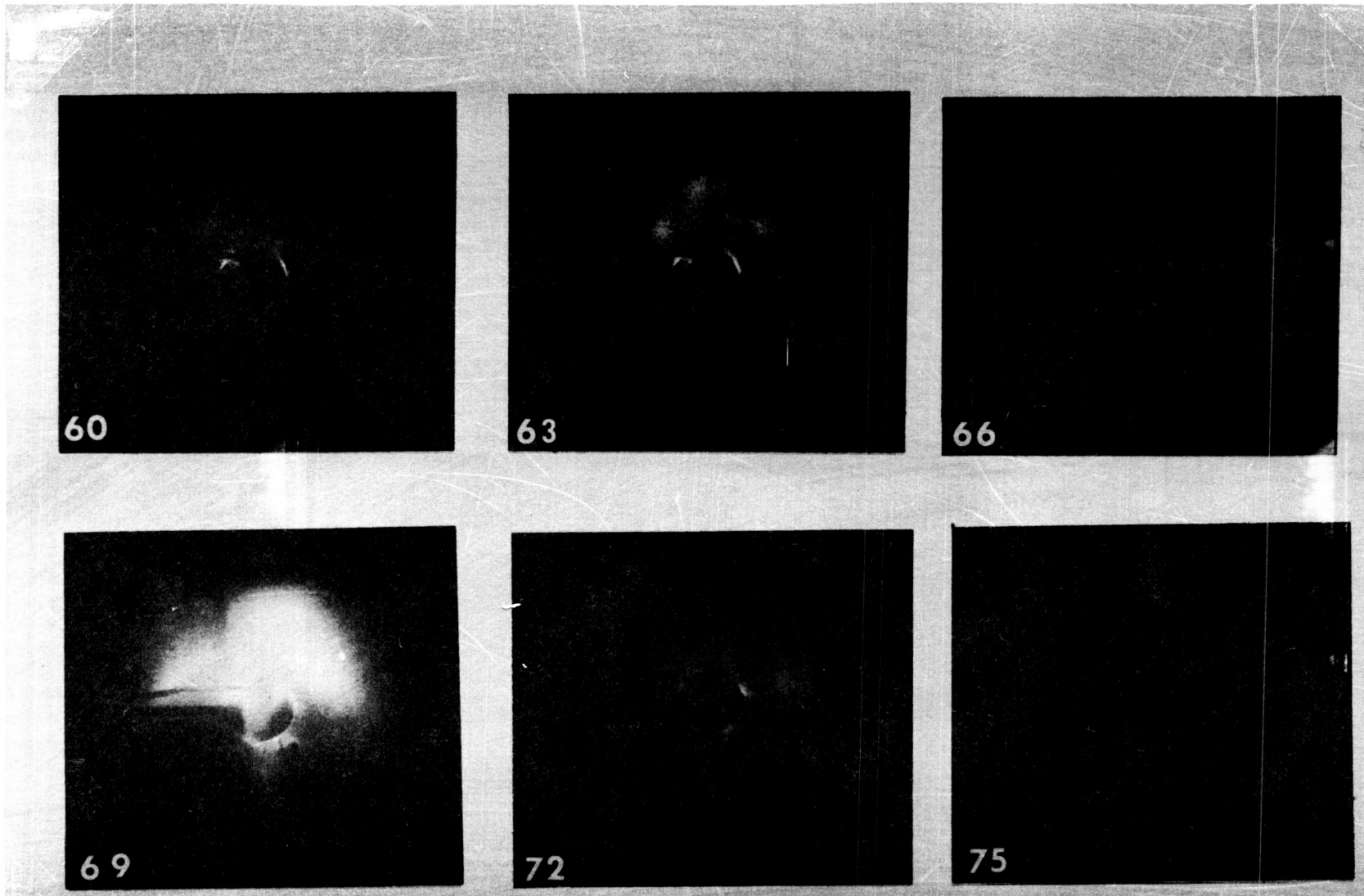

View from sunrise equatorial position of Solar Wind Magnetosphere Interaction. 1 μsec exposures. Numbers refer to time in microseconds from bank firing. Wind incident from top. Primary bank energy 1.7 kilojoules.

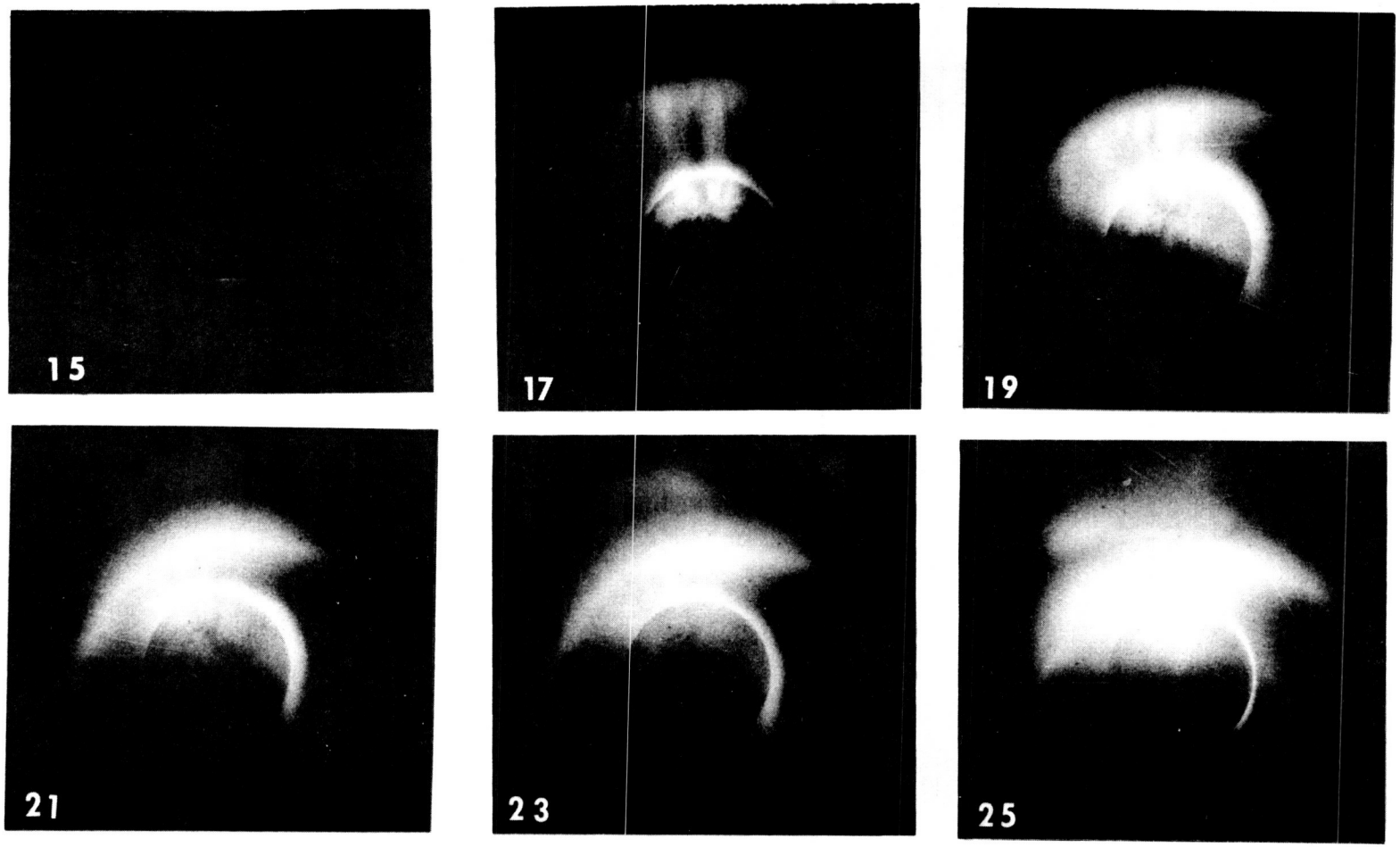

View from above polar axis of Solar Wind Magnetosphere Interaction. 1 μ sec exposures. Numbers refer to time in microseconds from bank firing. Wind incident from top. Primary bank energy 1.7 kilojoules.

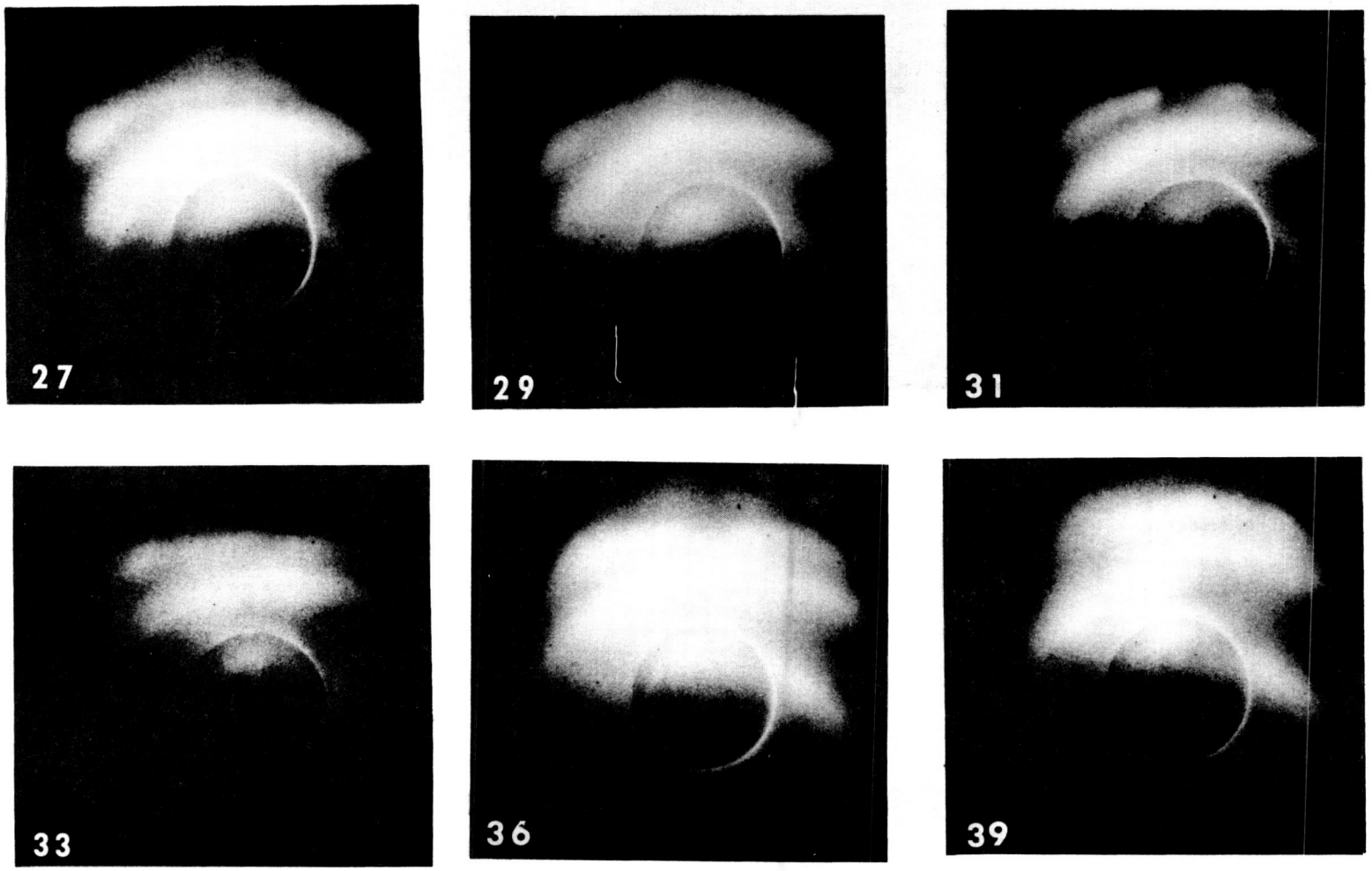

View from above polar axis of Solar Wind Magnetosphere Interaction. 1 μsec exposures. Numbers refer to time in microseconds from bank firing. Wind incident from top. Primary bank energy 1.7 kilojoules.

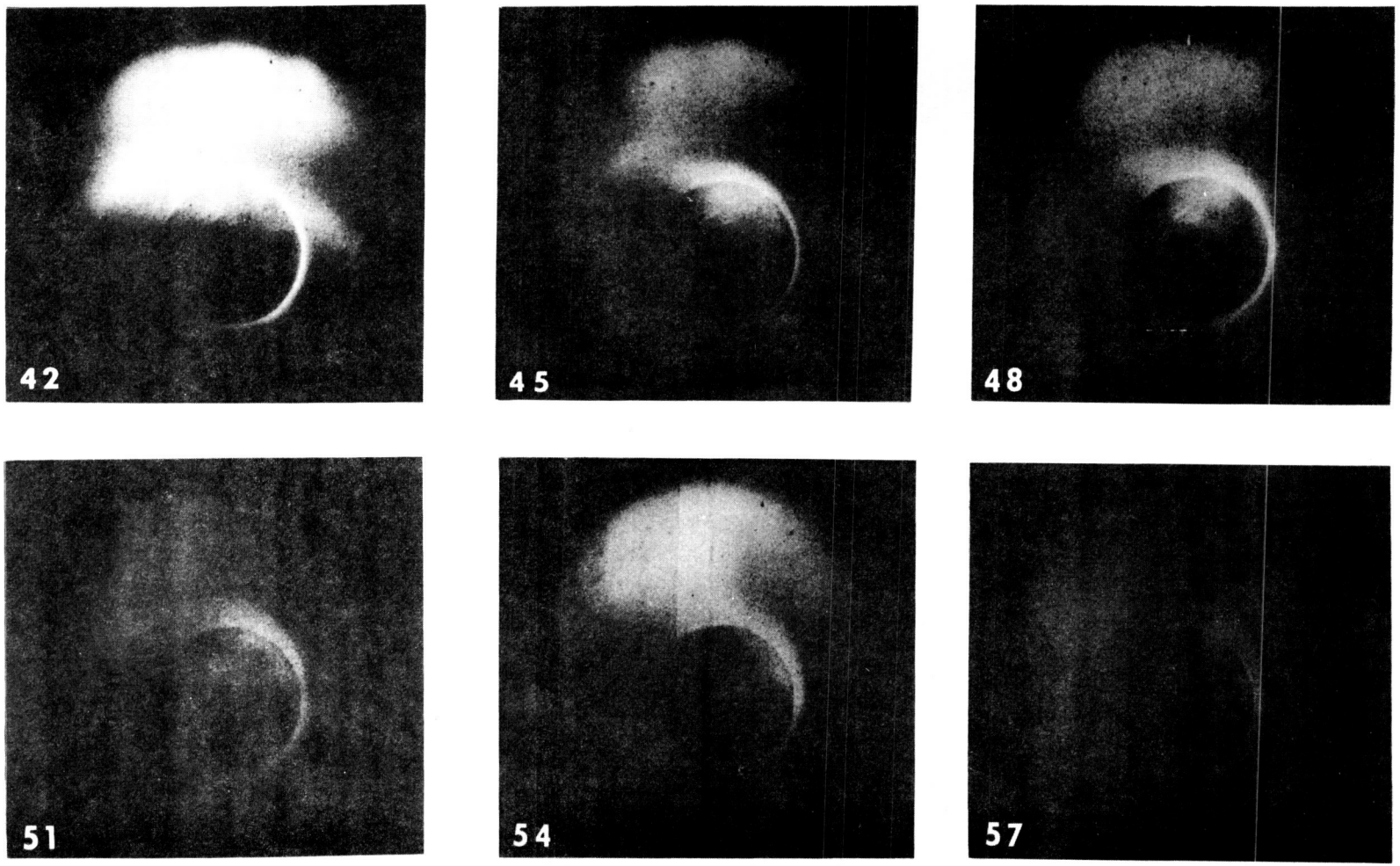

View from above polar axis of Solar Wind Magnetosphere Interaction. 1 μ sec exposures. Numbers refer to time in microseconds from bank firing. Wind incident from top. Primary bank energy 1.7 kilojoules.

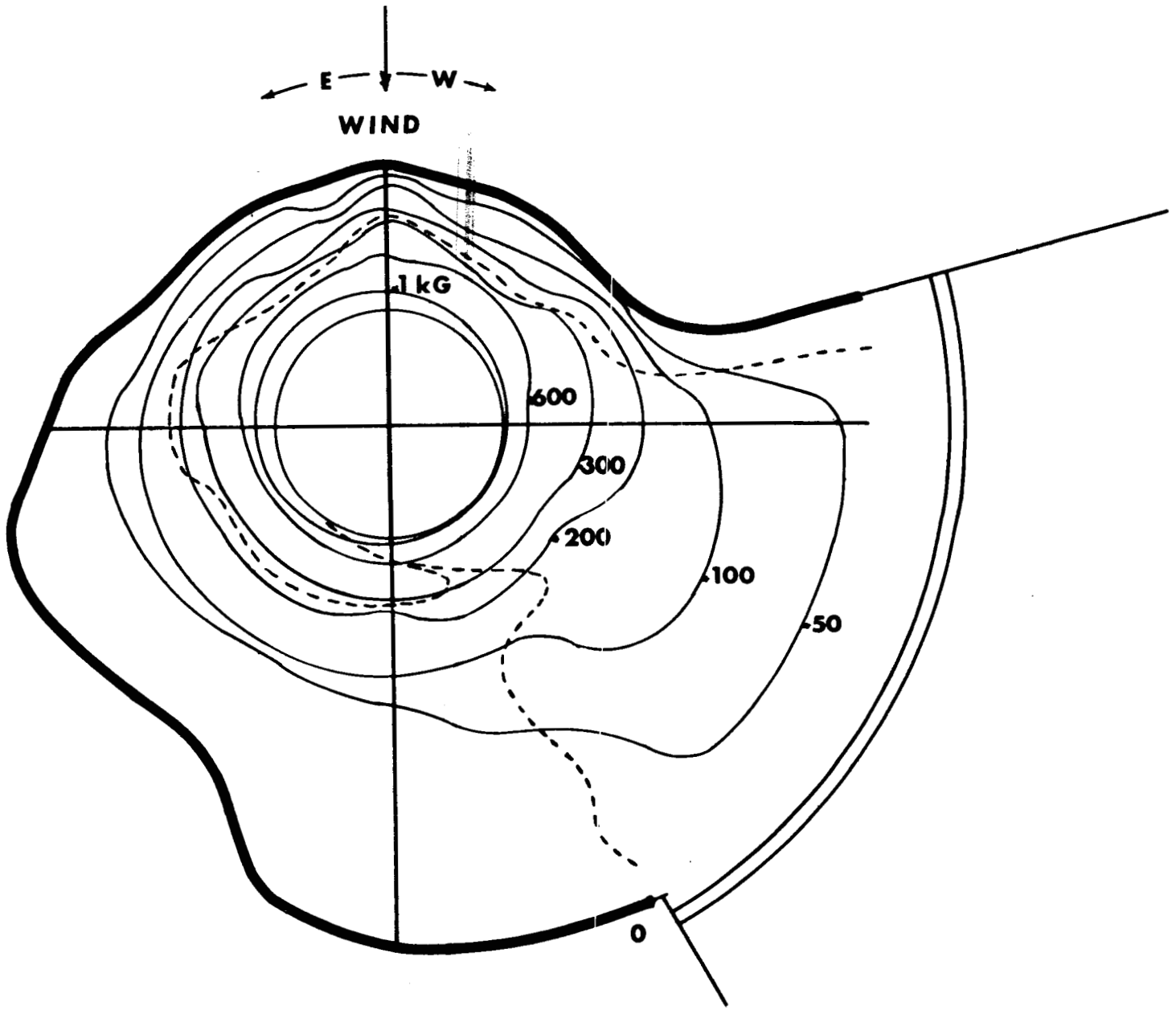

Figure 5 – Equatorial Magnetic Field (in gauss) at time of maximum boundary penetration. Dotted line shows contour of zero perturbation. Primary bank energy 1.7 kilojoules